buildings

MDPI

*Article*

# Influence of Infill on Reinforced Concrete Frame Resting on Slopes under Lateral Loading

**Pradeep Sivanantham [1,*], Subramanian Senthil Selvan [1], Satyanarayanan Kachabeswara Srinivasan [1], Beulah Gnana Ananthi Gurupatham [2,*] and Krishanu Roy [3,*]**

[1] Department of Civil Engineering, SRM Institute of Science and Technology, Chennai 603203, India
[2] Division of Structural Engineering, College of Engineering Guindy Campus, Anna University, Chennai 600025, India
[3] School of Engineering, The University of Waikato, Hamilton 3216, New Zealand
* Correspondence: pradeeps@srmist.edu.in (P.S.); beulah28@annauniv.edu (B.G.A.G.); krishanu.roy@waikato.ac.nz (K.R.)

**Abstract:** When compared to traditional reinforced concrete constructions on level surfaces, buildings situated on hills with slopes require additional consideration, particularly when seismic loading is an important factor. In hilly slopes, the ground-level columns of structures have different heights due to the nature of the slope, which leads to a short column effect. This paper represents an experimental and analytical investigation of the behaviour of reinforced concrete frames and their response in sloped regions of hills, in which global retrofitting techniques were adopted by providing solid infill in the short column effect zone for the columns in the same storey of differentheights. Numerical analysis was conducted on how infill affected the short column effect under lateral cyclic loads. It was discovered that compared to bare reinforced concrete frames, masonry infill greatly increased the lateral load-carrying capacity by up to 50%. In the meantime, the frame's ability to dissipate energy increased linearly. After infill was added to the frame with the short column effect, the reinforced concrete structure's different reactions, including ultimate load displacement, crack pattern, energy dissipation, and energy absorption, were examined. With the addition of a solid infill, the reinforced concrete structure's lateral strength and energy dissipation capacity were increased by 2.45 times. The damage development on the reinforced concrete frame with infill and the short column effect was less impacted by lateral stress than the reinforced concrete frame without infill.

**Keywords:** short column effect; hill slope; energy dissipation; sloped region; stiffness; seismic analysis; infill

check for updates

**Citation:** Sivanantham, P.; Selvan, S.S.; Srinivasan, S.K.; Gurupatham, B.G.A.; Roy, K. Influence of Infill on Reinforced Concrete Frame Resting on Slopes under Lateral Loading. *Buildings* **2023**, *13*, 289. https://doi.org/10.3390/buildings13020289

Academic Editor: Roberto Capozucca

Received: 13 December 2022
Revised: 7 January 2023
Accepted: 13 January 2023
Published: 18 January 2023

**Copyright:** © 2023 by the authors. Licensee MDPI, Basel, Switzerland. This article is an open access article distributed under the terms and conditions of the Creative Commons Attribution (CC BY) license (https://creativecommons.org/licenses/by/4.0/).

## 1. Introduction

In general, there are several earthquakes occurred in the past causing severe damage to life and structure throughout history. Earthquakes are a major concern as they will cause significant damage to the society if they are of high magnitude and intensity. Due to the nature of the terrain in the hill regions, most buildings now need to be built on a slope to decrease landslides by eliminating the earthwork, as well as to make it more cost-effective by building on the slope without excavating too much soil and fortifying the periphery to stop landslides. This may lead to variations in the heights of columns in the ground storey. Such columns that are short compared to that regular column in moderately steep slopes are called short columns. Since the columns are getting shorter due to the slope. Naturally shorter columns become stiffer and attract more lateral load. This leads to severe damage because of significant changes in the response to earthquakes, which is known as the short-column effect. Hence reinforced concrete (RC) framed structures on hill slopes are of great importance. Proactive disaster prevention is the process of adopting significant techniques and measures before the disaster occurs, so that future damage and loss to human life, as well as structure, can be prevented to a greater extent.

The reinforced short columns were laterally deflected by cyclic loading and the various amounts of reinforcement provided along longitudinal and transverse directions have a significant effect on the column under earthquake loading. The spacing of transverse reinforcement influences the rate of degradation of the hysteresis loop area, crack width control in the inclined direction of the column was achieved by resisting shear with the help of transverse reinforcement spacing [1]. An overview of the damage that reinforced concrete members sustains when subjected to significant inelastic cyclic loads similar to those encountered during a strong earthquake. The efficiency of a large number of damage indices proposed in the literature is explored and critically evaluated using the criterion of structural analysis and seismic risk assessment [2]. A multi-storey structure on the slope of the hill was investigated, and loads of buildings were moved to the hill slope at the foundation level. To determine the safety factor against the slope sliding failure, the building slope was analysed. The provision for the foundation in the slope has been computed and emphasised [3]. Buildings with various designs have been modelled and examined on various types of soil on slopes. The inelastic behaviour of macro-models of structural components, and two hysteretic models (a polygonal model and a smooth model) were devised. These models can be used to represent the deterioration of strength, stiffness, and bond slip over time. These models' theoretical foundations, development, and implementation are discussed. This article presents a comprehensive overview of one-dimensional inelastic material behaviour modelling, demonstrating how multiple hysteretic models are derived from fundamental principles of mechanics and thermodynamics via numerous assumptions that lead to approximations [4].

The major goals are to assess the contribution of carbon fibre reinforced polymer (CFRP) to the mechanical and energy performance of RC short columns that have been subjected to combined compressive and flexural loads. Short columns are subjected to shear stress during earthquakes due to their low resistance to large horizontal displacements. CFRP or glass fibre reinforced polymer (GFRP) was used to reinforce seven of the structures, either constantly or intermittently. Damage indices were generated to estimate the impact of the composite reinforcement's composition and geometry [5]. The reinforced concrete frame with an infill wall shorter the than column height was investigated. This generates a short column effect and the same was observed in many past earthquakes, An effective method of placing infill wall segments near the short column to prevent the failure due to shear was adopted and investigated. A parametric study is carried out for a one-storeyed infill frame first and the same is extended to multi-storey buildings damaged due to the short column effect in Turkey. The results show that short columns with infill segments in the surroundings reduce the shear force effectively [6,7]. The analytical investigation was adopted to find the peculiar behaviour of hill buildings under seismic load, and then the dynamic behaviour of such buildings is compared with flat ground buildings in terms of displacement, drift, fundamental natural period, shear, and plastic hinge formation [8–10]. The seismic performance of a four-story, two-bay high-performance concrete frame (HPC) was studied. On a 1/5-scaled HPC frame, low reversed cyclic loading was performed. The failure pattern, failure mechanism, deformation restoring capacity, displacement ductility, and energy dissipation capacity of the framed specimen were all examined [10]. The strength and behaviour of reinforced concrete (RC) frames with ferrocement infills were investigated experimentally. A 1/4 scaled-down model of one bay-three-storey frame was evaluated under reversed cyclic lateral loading for this purpose. The hexagonal wire mesh used in the ferrocement infill has different volume fractions of mesh reinforcement: 0.20%, 0.30%, and 0.40%. Frames with ferrocement infill were compared to frames without infill in terms of strength and behaviour. The strength, stiffness, energy dissipation capacity, and ductility of frames with ferrocement infill were greatly enhanced as compared to the bare frame, according to the experimental results [11].

An analytical study of the behaviour of RC frames in sloped regions was carried out, in which three different techniques are incorporated to alleviate the short column effect under cyclic loadings, such as equating the stiffness of the columns to that of the stiffness of

the short column, thereby changing the cross-section of the columns, providing infill, and providing steel plates at regions of maximum shear [12]. Incremental inelastic dynamic damage studies on multiple MRRCFs under twenty seismic ground motions to anticipate the influence of masonry infill panels on the imposed damage of moment-resisting reinforced concrete frames (MRRCFs) under earthquake excitation were investigated [13]. A detailed experimental and numerical investigation was conducted to demonstrate its efficacy and efficiency over the conventional brick infill system. The energy-dissipating hysteretic infill functions as a passive energy dissipation system that has several advantages over traditional infill, including the arrest of diagonal compressive strut creation, a stable post-yield behaviour for the infilled frame, and a better failure mechanism. Under uniaxial in-plane loading, out-of-plane loading, and simultaneous bi-axial loading, the performance of the energy-dissipating hysteretic infilled frames is examined, taking into account the effect of opening [14]. A numerical investigation was carried out into the progressive collapse mechanisms of steel frames with partial infill walls under fire scenarios. The load redistribution and collapse mechanisms of steel frames exposed to various fire scenarios (edge bay and central bay fires) are investigated. The effects of partial infill wall strength, opening percentage, and layout are also investigated. According to the results of the numerical analysis, partial infill walls create combined tensile force and bending moment at the ends of surrounding beams [15]. The link between bricks and mortar is presumed to be unbroken at the moment of brick or mortar breakdown in failure theories for masonry under compression. These failure models do not adequately account for how bond strength affects masonry compressive strength. Through an experimental program employing local bricks and mortars, the impact of bond strength on masonry compressive strength has been investigated in this study [16]. The new models, which depend on building height and the story mass of the intermediary levels, have been constructed for both bare and infilled frame configurations. For new structures, the mass of intermediate floors is a quantity that is simple to define and might be seen as including the mass of the building under analysis as well as the other stiffness characteristics often used for calculating the value of T. The formulations that have been proposed have been contrasted with those from technical codes and scientific literature, demonstrating the correctness of the models and their ability to offer a fair level of coverage in the T forecast for various building H values [17].

This article discusses the infilled frame with strut under specified loads as well as partial interface materials. As part of the study, the infilled frame with various partial interfaces will also have its elastic behaviour and dynamic properties under monotonic in-plane loading evaluated. The critique focuses on the twenty-five frames' lateral rigidity in contrast to partial interface frames. The findings from this criticism can help with future research on partial interface materials [18]. Experimental and numerical research are used to examine the nonlinear behaviour of integral infilled frames, in which the infill and the frame are joined by a variety of interface materials. Two-bay and three-story reinforced concrete frames with and without infill were used for the experiments against static cyclic stress, which were done at a size of one-sixth. Infilling made the bare frame more rigid, and the amended frame's strength rose by 20% over the bare frame. The modified infilled frame has a 42% higher ductility ratio than the standard infilled frame [19]. To conduct a nonlinear analysis on a six-story frame, seven near-field signals scaled by the design spectrum of the Italian code (NTC, 2008) have been used. The response has also been established for the same frame shielded twice—once with base isolators and once with hysteretic-type energy dissipators. The objective of the study is to gather quantitative information about the impacts of near-field ground motion on frame structures and on the damage to them even when passive seismic protection devices are present [20].

The studies mentioned above show that the majority of research focuses on improving the stability and strength of structures. Understanding how infill affects the seismic performance of RC frames with a short-column effect is the primary goal of this work. The seismic performance of the RC frame with and without infill under lateral cyclic loading was examined experimentally for this purpose. The short column effect with and without

infill served as the major research variables. Experimental research was done on the fracture pattern, energy dissipation, peak load, and displacement.

## 2. Experimental Investigation

To determine the behaviour of RC frame short column effect on the structure under lateral loading in hilly regions with and without Infill. An experimental investigation is carried out for two bare frames of which one is an RC frame having columns of different heights on the same storey without infill and the second frame is a reinforced concrete frame having columns of different heights on the same storey with infill. The experiments were carried out on one-sixth scale two-bay and two-storey reinforced concrete frames with and without infill against cyclic loading based on literature review and laboratory conditions [21]. This section presents the details of the experimental investigation.

### *2.1. Geometric Specifications and Material Properties*

The M25 concrete grade and Fe 415 grade steel were selected based on previous case studies after conducting physical and mechanical properties tests on steel and concrete [22,23]. From the literature review and laboratory loading conditions, the loading conditions are selected to determine the failure load and pattern of cracks.

The foundation slope is provided at a slope of 9° as per the measurements taken from satellite views of google earth pro for SRM University, Sikkim Campus, India. Where the slope is measured for the range of distance 50 m with a minimum elevation of 1173 m to a maximum elevation of 1181 m, as shown in Figure 1a. The RC foundation is provided with a length of 1300 mm and a depth was 200 mm. Total depth varies from one end of 300 mm to 500 mm at another end, as shown in Figure 1c. In foundation 6 numbers of 12 mm, diameter bars are provided as the main reinforcement and the transverse reinforcement of 8 mm diameter are provided at 100 mm c/c spacing with a clear cover of 20 mm, as shown in Figure 1d. Meanwhile, the column of size 100 mm x 90 mm is provided with 4 numbers of 6 mm diameter longitudinal reinforcement and transverse reinforcement of 6 mm diameter at 30 mm c/c spacing with a clear cover of 10 mm. The Beam of size 90 mm $\times$ 100 mm was provided with 4 numbers of 6 mm diameter longitudinal reinforcement and transverse reinforcement of 6 mm diameter at 50 mm c/c spacing with a clear cover of 10 mm. For the reinforced concrete frame with infill, the infill was constructed by using normal clay brickwork and mortar, as shown in Figure 1b. In India, hand moulding is commonly used to create burnt clay bricks, which are subsequently burned in kilns. Locally accessible burned clay bricks have been evenly spread over all four bays. The second-class brick of compressive strength 7.5 N/mm$^2$ was used for the construction of masonry walls.

To prepare mortar that complied with IS 12269 [24], regular Portland cement was employed. The rich mortar of 1:4 mix ratio was used with a constant water-cement ratio of 0.56 to maintain workability, and then the strength of the mortar is 30 N/mm$^2$ for 28 days of curing. The material properties such as the grade of concrete and steel used in the foundation are similar to that of the reinforcement used in the column and beam.

### *2.2. Experimental Setup for Testing*

The two specimens were hauled in a similar pattern to the loading frame with the help of a crane in the A-type self-straining 3D loading frame as represented in Figure 2. The specimen is fitted with two base plates on both sides with 8 mm size bolts. The specimen is held tight at the base by providing channels on either side and thus tested by applying load by utilizing a hydraulic jack for the push and pull of the frame for the full repeated loading. A hydraulic push-and-pull jack is adopted with a pumping unit having a capacity of 200 kN. The jack is attached to a universal load cell of capacity 100 kN. These are attached with a load indicator. For effective transfer of load, the loading cell is attached to a hinged type. Linear variable differential transformer (LVDT) of 100 mm push–pull capacity (50 mm push and 50 mm pull) connected to the displacement indicator of 100 mm capacity is fitted

along two storeys to calculate the deformations. The complete test setup of investigating the reinforced concrete frame is shown in Figures 3 and 4a.

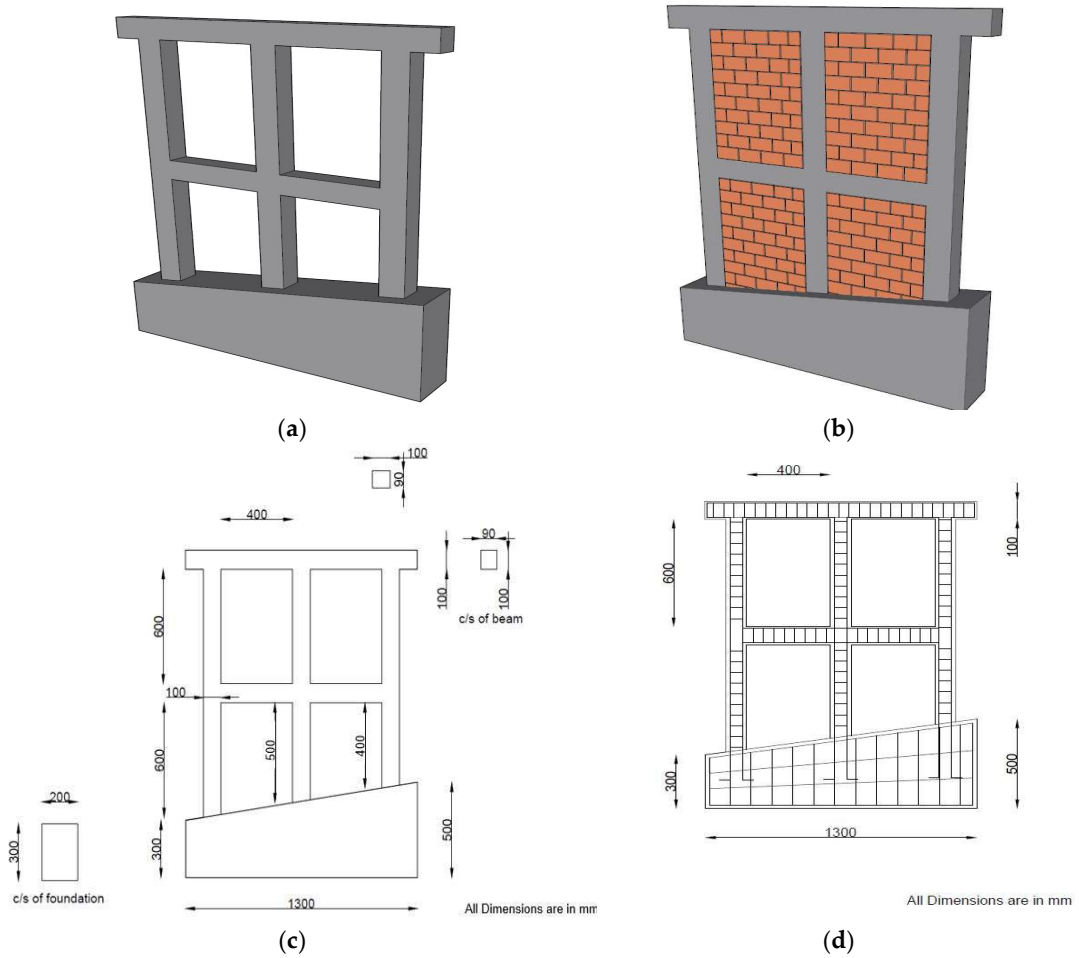



**Figure 1.** Geometric representation of a reinforced concrete frame. (**a**) Sloped reinforced concrete bare frame. (**b**) Sloped reinforced concrete infill frame. (**c**) Geometry of a reinforced concrete frame. (**d**) Reinforcement position of a reinforced concrete frame.

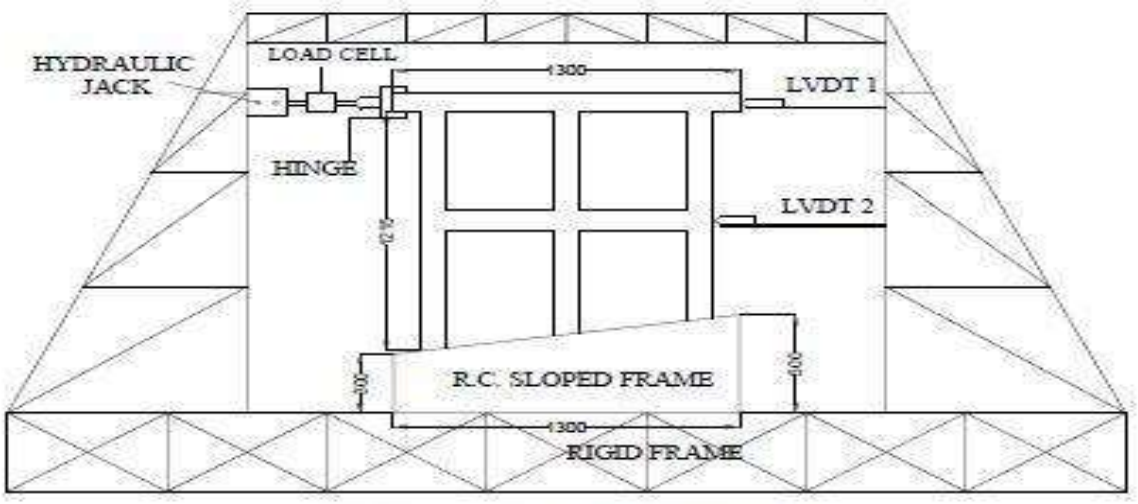
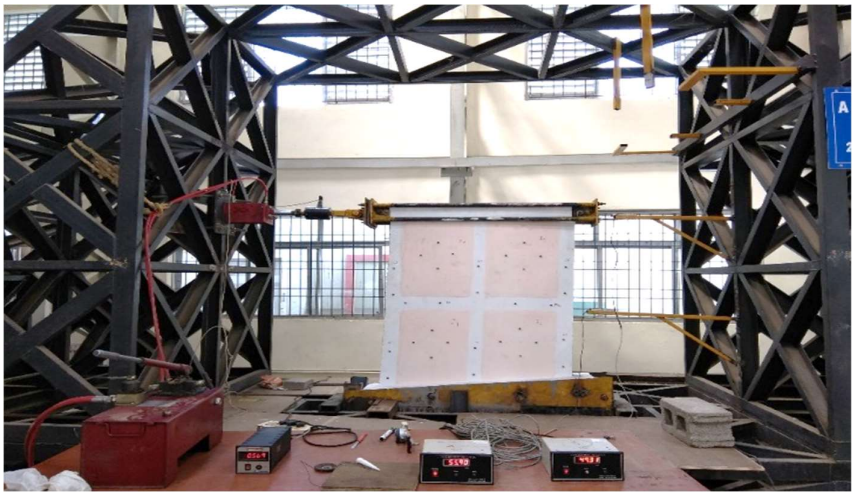


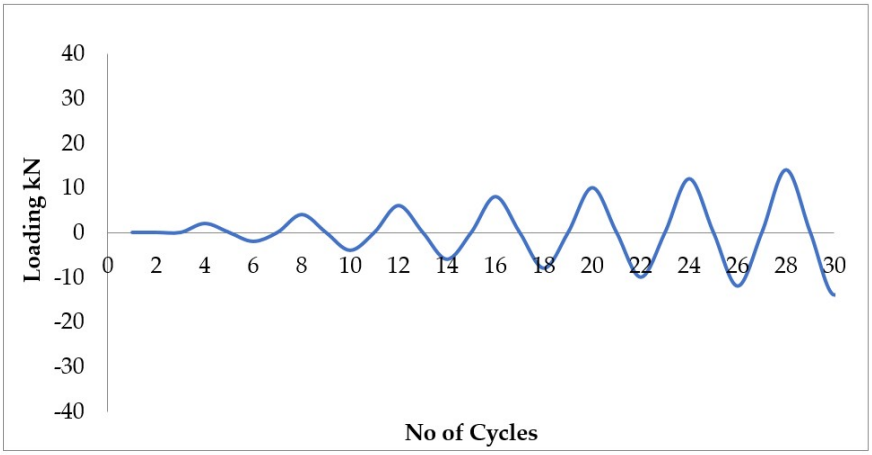

**Figure 2.** Schematic representation of a self-straining frame.



**Figure 3.** Experimental setup of a sloped reinforced concrete bare frame.



(**a**)




(**b**)

**Figure 4.** (**a**) Experimental setup of the self-straining frame with a sloped reinforced concrete infilled frame. (**b**) Loading pattern.

The horizontal reverse cyclic loading was applied through the 100 kN capacity load cell at an interval of 2 kN per cycle until the specimen achieves the failure load, as shown in Figure 4b. The loading pattern will be terminated once the specimen reaches the ultimate lateral load-bearing capacity or severe damage occur on the specimen. Bricks

used for constructing the masonry wall were pre-wetted and cut into required sizes using a cutter machine. The geometry of the bricks piece used for the masonry wall was 100 mm × 75 mm × 65 mm. Rich mortar of 5 mm thickness is used between the bricks to maintain good bonding.

### *2.3. Brick Masonry Testing*

Brick masonry's compressive strength was evaluated through five-brick-high bonded prism stacks with a height-to-thickness ratio of 3.45. Prewetted prism bricks were connected with rich mortar of 5 mm thickness throughout the span, as shown in Figure 5a,b, and they were kept in wet burlap for 28 days of curing. The rich mortar of ratio 1:4 was used to enhance the bond strength of the masonry prism. An increase in bond strength leads to an increase in compressive strength, hence the compressive strength of 6.82 N/mm$^2$ observed from the testing shows the increase in masonry prism strength.

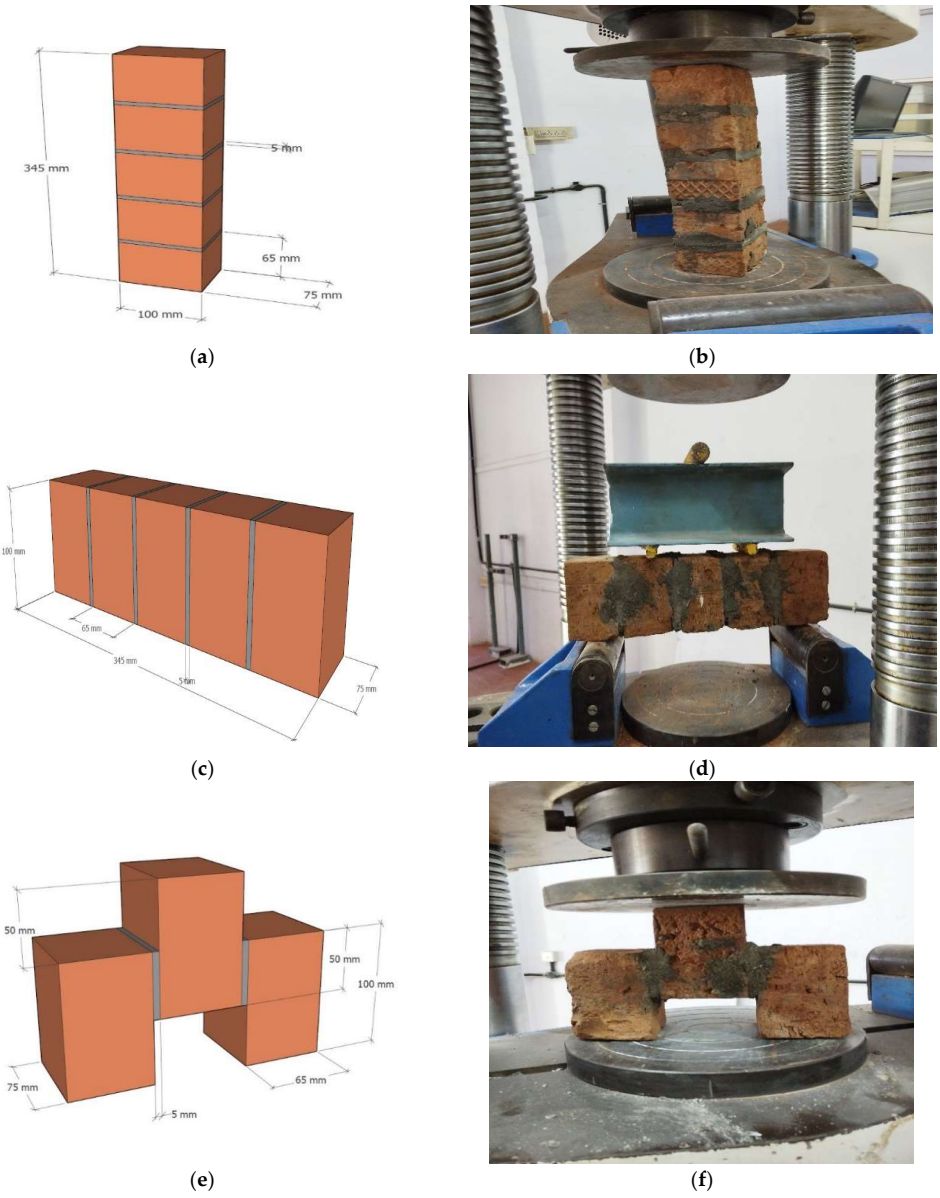



**Figure 5.** Brick masonry testing setup and specimens. (**a**) Schematic representation of five-brick-high bonded prism stacks for a compression test. (**b**) Brick-high bonded prism stacks for a compression test. (**c**) Schematic representation of five-brick-high bonded prism stacks for the flexure test. (**d**) Brick prism stacks for the flexure test. (**e**) Schematic representation of prism stacks for the shear test. (**f**) Brick prism stacks for the shear test.

Through five-brick-high bonded prism stacks with a length-to-thickness ratio of 3.45, the compressive strength of masonry was assessed. The flexural bond strength of brick masonry was determined by testing the specimen in two-point loading with a simply supported setup placed in a servo control compressive strength test machine, as shown in Figure 5c,d. The flexural strength of brick is 0.72 N/mm$^2$.

To measure the shear bond strength of the brick mortar joints, a brick triplet specimen was employed. Figure 5e,f the test setup is displayed. This illustration clearly shows that the top and bottom bricks' horizontal mobility was constrained, while the centre brick's movement was unrestricted. The load was applied through the hydraulic jack of the servo control compression testing machine gradually until the bond between the brick and mortar joint ruptured from which the shear bond strength could be calculated. Due to the increase in flexural bond strength, the significant increase in the shear strength is 0.91 N/mm$^2$, as shown in Table 1.

**Table 1.** Strength of brick masonry.

| Type | Prism Compressive Strength (N/mm$^2$) | Flexural Bond Strength (N/mm$^2$) | Shear Bond Strength (N/mm$^2$) |
|---|---|---|---|
| Brick Masonry | 6.82 | 0.72 | 0.91 |

As the bond strength is raised, the masonry prism begins to collapse due to diagonal shear cracks developed, as seen in Figure 6. This failure is comparable to diagonal failures in compressed concrete cylinders. Additionally, it can be seen that the connection does not fail in these prisms. Hence, the high bond strength brick masonry with rich mortar is used inside the frame as an infill to take the lateral load.



**Figure 6.** Masonry diagonal shear failure under compression.

### *2.4. Modulus of Elasticity*

By applying uniaxial compression to the cylinder specimen and measuring the deformations with a dial gauge positioned between the 100 mm gauge length, as shown in Figure 7, the modulus of elasticity was computed. A compressometer was used to conduct the test by IS 516-1959 [25]. The 200 mm × 100 mm cylinder specimens were mounted on compression testing apparatus, and the stress was applied until the cylinder collapsed. For each increment, the target load and deflection are measured.

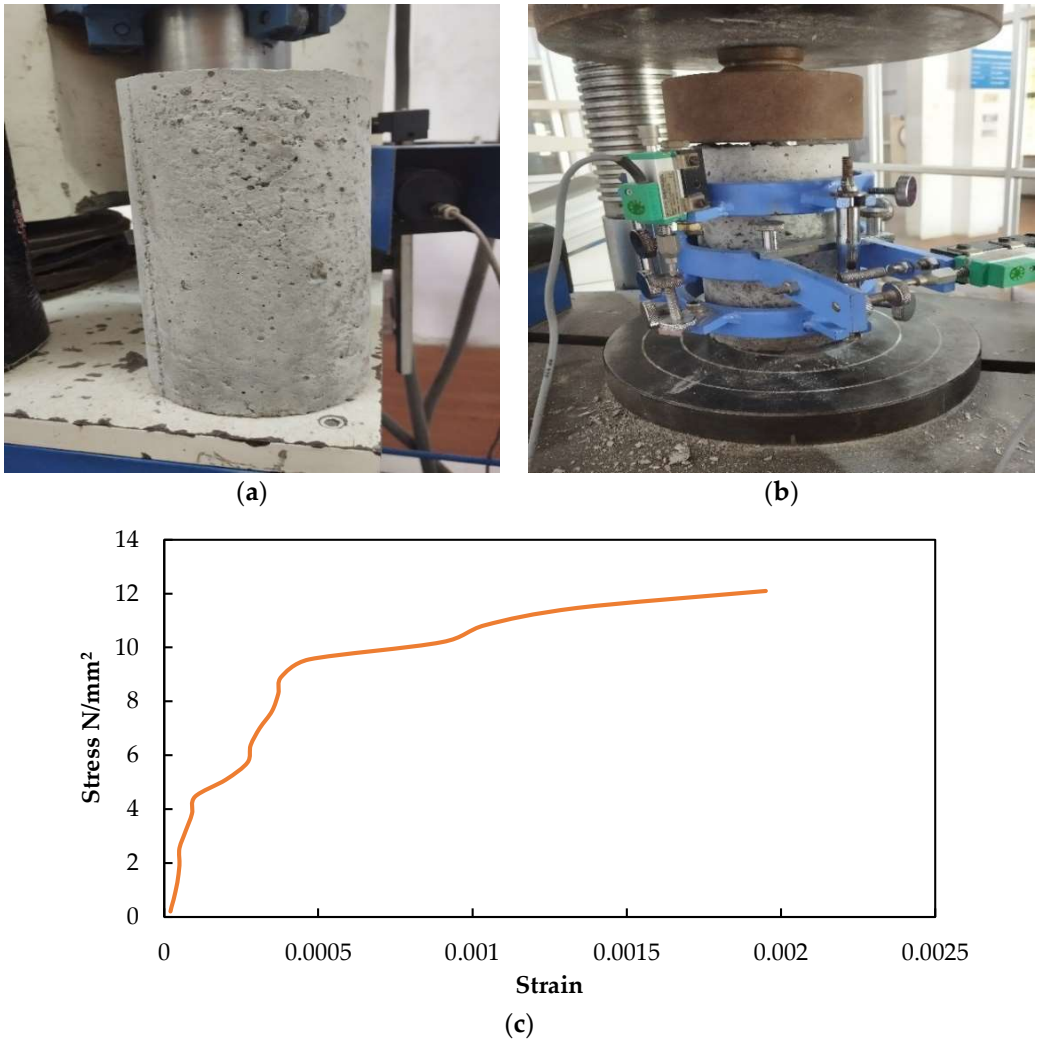



**Figure 7.** Compressometer test for the lateral strain and linear strain measurements. (**a**) Cylinder specimen, (**b**) compressometer test setup, and (**c**) Stress vs. strain curve for M25 conventional concrete.

Based on the change in lengths, the deflection values were calculated from the strain value. Divide the applied load by the cylinder's cross-sectional area to compute the stress, then divide the dial gauge readings by the gauge length to determine the strain. To determine Young's modulus of the standard concrete specimens, various loads' deformation was measured. The computed modulus of elasticity for conventional concrete was $25 \times 10^3$ N/mm$^2$. Meanwhile, the change in diameter concerning the diameter measured through the extensometer leads to finding lateral strain. Hence the ratio of lateral strain to linear strain provides the poison ratio of 0.2 for concrete. Analytical modelling inputs are based on the outcomes of the material properties based on the compressometer test, as shown in the Figure 7a–c.

### *2.5. Hysteretic Behaviour*

The lateral load-displacement hysteretic curve for conventional reinforced concrete frame with short column effect and Infilled reinforced concrete frame with short column effect is shown in Figure 8a,b. The loading and displacement at the initial stage show a linear relationship. So that the area of the curve till that stage is narrow and small. The loading is further continued till the column enters into an elastoplastic state where the extension of cracks and yielding of steel takes place. This observation shows that the slope in the hysteretic curve gradually decreased, and the area of the curve increased.

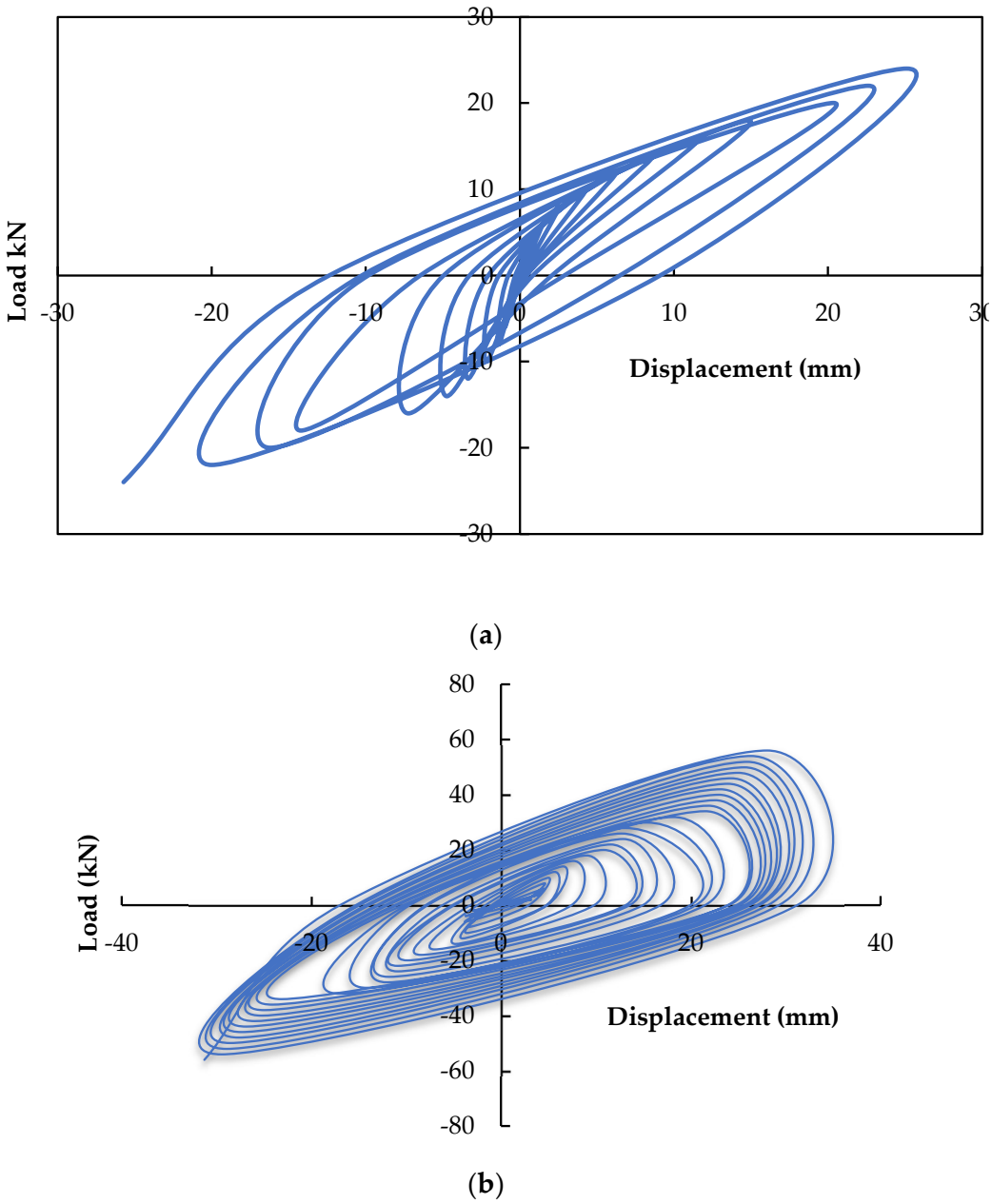



**Figure 8.** Hysteretic curve. (**a**) Bare frame. (**b**) Infill frame.

When the lateral load is removed, the specimen shows residual deformation to different extents. The plastic deformation and damage accumulation are reflected very clearly near the joints and supports of the conventional reinforced concrete frame at peak load. In post-peak, load stage hysteretic response was very poor due to the very fast strength attenuation of the specimen and the brittleness of concrete. While comparing with longer columns on the same floor shorter columns attract more force and all of a sudden brittle failure is observed and this is favourable for the collapse of structures during strong earthquake motion. In contrast, a conventional reinforced concrete frame with infill and short column effect shows excellent response and the strength degradation is also slow due to the increase in stiffness, which reduces the displacement and improved the performance of the structure.

Once the infill is provided inside the frame the hysteretic behaviour becomes more stable and the area of the hysteretic loop was larger. Subsequently, with an increase in lateral load and displacement, the lateral strength of the frame dropped insignificantly after

the failure take place in the supports and joints of the columns. However, for the frame without infill, the hysteretic behaviour is less stable, and the area of the loop is also small. After reaching the ultimate load the lateral strength declined significantly.

The peak load capacity and horizontal displacement profiles of frames reveal the high stiffness capacity of the frame during the pulling and pushing process. Meanwhile, a slight discrepancy between the pulling and pushing profiles can be observed because of the combined damage effect. The ultimate load capacity for a bare frame is 27.9 kN in the case of push (positive), while in the case of pull (negative), it is 26.5 kN. For an infilled sloped frame, it is 60 kN in the case of push and 57 kN in pull. The maximum displacement of the bare frame is 37 mm at the ultimate load of 27.9 kN. At the failure load of 30 kN, the bare frame achieves a maximum displacement of 50 mm. The displacement of the Infilled frame at the same load of 27.9 kN is 13.1 mm, which is less compared to the bare frame. However, the maximum displacement of the infilled frame is 28 mm while it has reached an ultimate load of 60 kN. Due to the improved stiffness by the provision of masonry infill and rich mortar with significant bond strength the infilled frame resists the lateral load to a higher extent.

### *2.6. Crack Pattern and Failure Pattern*

Cracks in the supports and beam-column joints opened and gradually evolved under cyclic reversals. Crack width and length increased with increasing drift amplitudes, propagating from the beam-column joints to an approximately mid-height of the column. This propagation resulted in a partial expulsion of the concrete first at the joints of the short column. A similar damage pattern developed on the other floors causing the concrete to crush at the interior and exterior sides of the columns. When the frame reaches its maximum load, the bare frame exhibits shear fractures at joints that are 6 mm broad and that open out at the support of a short column. When the masonry infill is installed, the scene in the second specimen is completely altered. Even though shear fractures are not forming close to the joints and supports, the load transmission across the brick masonry has caused cracks and failures that are evident.

The crack width observed in the frame started developing as the loads were increased gradually. At the initial load, very thin cracks of 2 mm are seen near the joints of the short column. The initial crack for a normal sloped reinforced concrete frame was obtained at 8 kN. Meanwhile, for the reinforced concrete frame with infill, the cracks evolved slightly at 14 kN. The initial crack for the reinforced concrete sloped frame is seen as a hairline crack. The ultimate failure occurs at 26 kN and 59 kN for bare and infilled frames respectively with a gap developed between infill and column along with the formation of diagonal cracks in brickwork. A crack width of 3 mm is observed near the support of the short column for the infilled frame. Crushing and spalling of bricks and concrete also took place near the joints and supports of the frame due to lateral movement of the frame, as shown in Figure 9.

### *2.7. Energy Absorption and Energy Dissipation*

Energy dissipation estimates, by the traditional area-based approach. In particular, Table 2 indicates the cumulative energy dissipated by each cycle at different levels, obtained as the area enclosed by a complete hysteresis loop for both pull and push. During the early loading process, energy absorption and dissipation of the frame increases gradually for both the bare frame and the infilled frame. The area beneath the hysteresis loops from the load vs. deflection diagram was used to compute the energy dissipation throughout various load cycles and the area within the cycles is used for evaluating absorption. A reinforced concrete frame with a short column effect when provided with the solid brick infill inside the bays shows tremendous improvement in the energy absorption capacity.

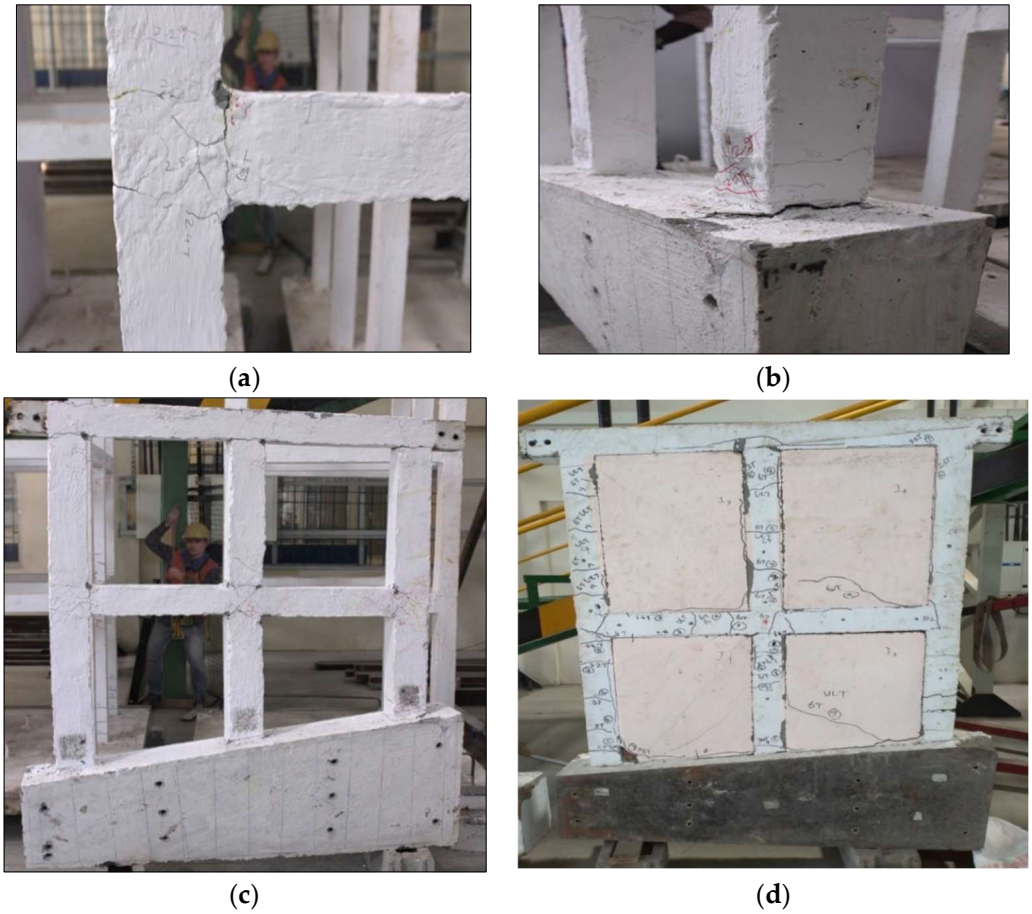


**Figure 9.** Evaluation of the damage and crack formation. (**a**) Joint failure (**b**) Support failure (**c**) Bare frame failure (**d**) Infilled frame failure.

**Table 2.** Energy absorption and dissipation for the bare frame.

| S.No. | Description | Bare Frame | | Infill Frame | |
|---|---|---|---|---|---|
| | | Push (J/kg) | Pull (J/kg) | Push (J/kg) | Pull (J/kg) |
| 1 | Energy Absorption | 34,428 | 21,439 | 84,344.3 | 64,362.5 |
| 2 | Energy Dissipation | 15,000 | 16,250 | 35,000 | 47,500 |

The energy absorption capacity of the reinforced concrete frame with infill is 2.45 times greater than that of the bare frame without infill. Energy dissipation of the infilled frame also increased significantly when compared to the bare frame. Due to the tiredness of the specimen while pulling after push the energy dissipation capacity of both frames decreased significantly.

To evaluate the effect of infill on the response of the reinforced concrete frame on slope quantitatively, the ratio of energy dissipation and absorption capacity of the reinforced concrete frame with infill to that of the reference frame without infill was proposed and calculated. The effect of infill on the energy dissipation capacity of the reinforced concrete frame was most remarkable on both push and pull, as shown in Figure 10. The energy absorption capacity of the reinforced concrete frame has almost doubled after the provision of infill. which can be quantitatively observed in the bar chart shown below in Figure 10.

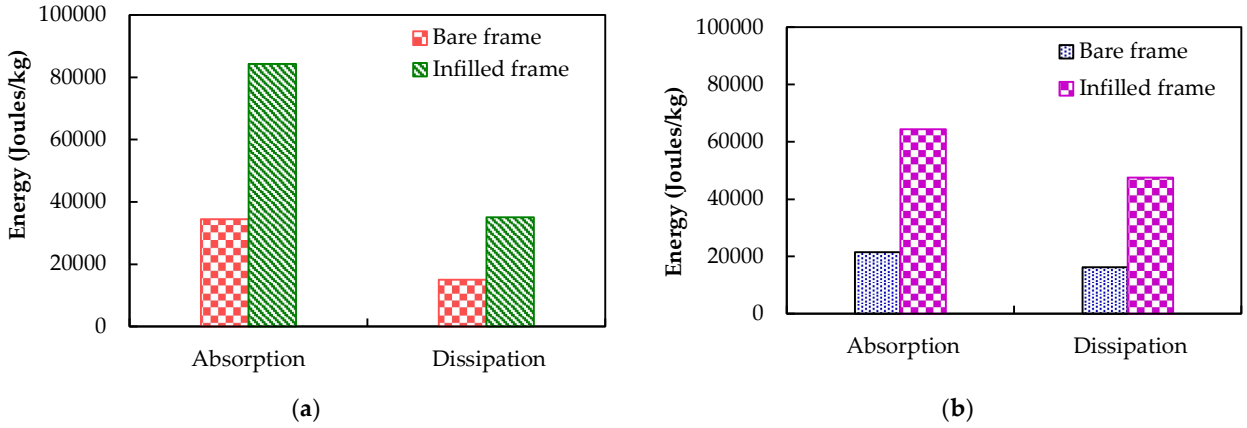



**Figure 10.** Energy absorption and dissipation of reinforced concrete frames. (**a**) Comparison of energy in the frame (Push). (**b**) Comparison of energy in the frame (Pull).

## 3. Analytical Investigation

Finite element modelling was done for both reinforced concrete bare frame and infilled frame using ABAQUS [26], as shown in Figure 11a,b. The material properties of M25 for concrete and Fe415 for steel were given as input. Rectangular-type meshes are considered based on the linear geometry of the column, beam, and foundation. Quad 3D element type is used to model square and rectangular type meshes. To connect the concrete and reinforcement in the finite element model, the embedded connection was used. At the same time to connect the concrete and mesh tie connection was used. The mesh size is optimised for the whole section. Utilizing various mesh sizes while applying the same load allowed for the analysis of the convergence research. Convergence was examined using the mesh sizes of 200 mm, 150 mm, 100 mm, 75 mm, 50 mm, 40 mm, 30 mm, 20 mm, and 10 mm. The convergence graph is produced, as shown in Figure 11c, using the results of the load and displacement for each size. When the linear pattern of the line moves in the graph, the value is recorded. For the investigation, a linear pattern of line forms with mesh sizes ranging from 75 mm to 20 mm and a higher-end convergence value of 75 mm was selected.

The material properties are taken based on the experimental investigations, young's modulus and Poisson ratio are derived from the compressometer test for the cylinder as 25 N/mm$^2$ and 0.2 respectively. The rich mortar of ratio 1:3 is adopted to create higher bond strength between bricks in masonry work. Hence the flexural bond strength and shear bond strength significantly increased along with the masonry compressive strength, which will extend the failure of masonry in lateral loading. Young's modulus of brick masonry work is considered as 2750 N/mm$^2$ and the Poisson ratio as 0.32. Then the lateral cyclic loading [27,28] is applied at the left top joint, and loading iteration was maintained evenly for both the frame as 150 kN, and the results are observed. Results are taken in the form of a hysteresis curve and stress deformation, as shown in Figures 12 and 13 through post-processing.

Stress deformation demonstrates unequivocally that for a sloped bare frame, the largest intensity appeared around the support and joints. When full masonry filling with rich mortar is applied, massive energy is dispersed in the masonry and the resistance to failure is greatly increased. The hysteresis curve displays the same behaviour as the actual inquiry, where the complete infill frame extends up to 57 kN with a displacement of 14.5 mm and the bare frame fails at about 26 kN with a frame displacement of 30 mm. The stiffness of the infilled frame reduced the displacement drastically, as shown in Figure 13. While compared to the bare frame the global retrofitting with full masonry infill shows very less displacement. Concerning the grade of concrete, displacement and load have been observed. The area under the hysteresis curve of the bare frame is relatively less compared to that of the infilled frame. The displacement observed in the hysteresis loop is linear before the failure of concrete until the frame is in the elastic stage. The hysteresis

loop became nonlinear once the specimen started failing, and also, the slope in the loop decreased as the displacement started increasing. In the bare frame, the slope started decreasing when the frame reached 23 kN, and slopes started falling after 50 kN in the masonry infilled frame.

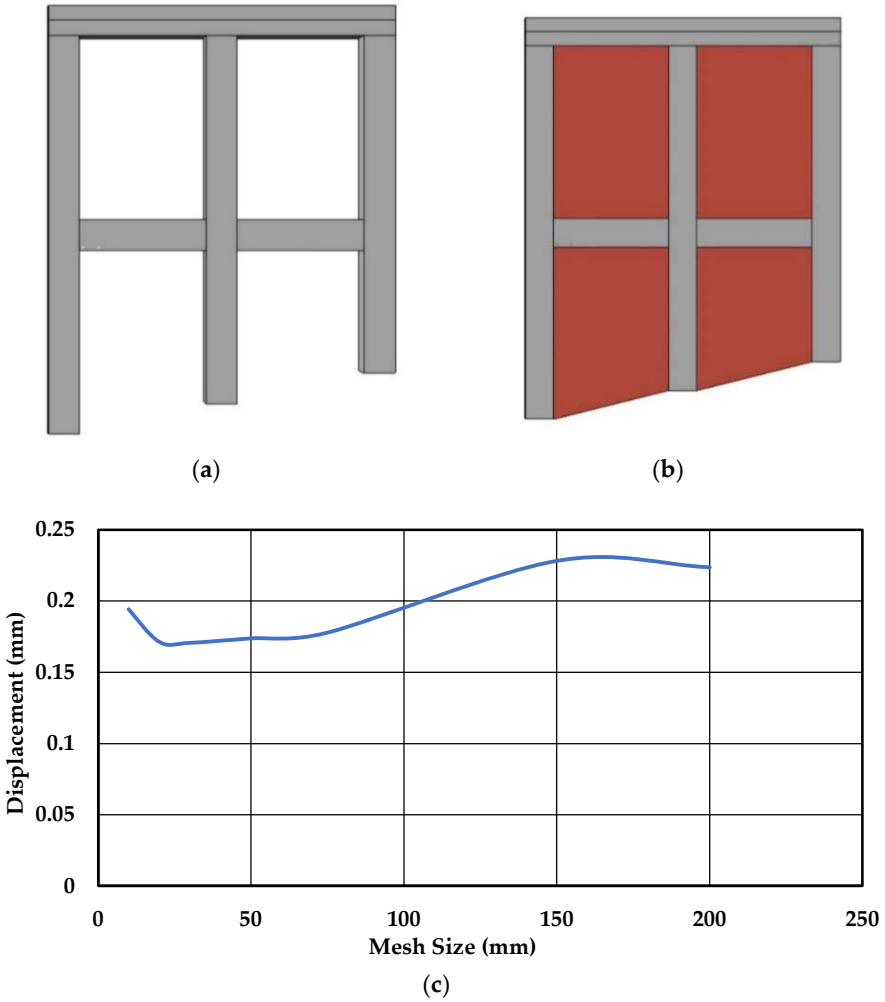



**Figure 11.** Finite element modelling of a reinforced concrete frame and convergence graph. (**a**) Bare frame on a slope, (**b**) infill frame on a slope, and (**c**) convergence study graph.

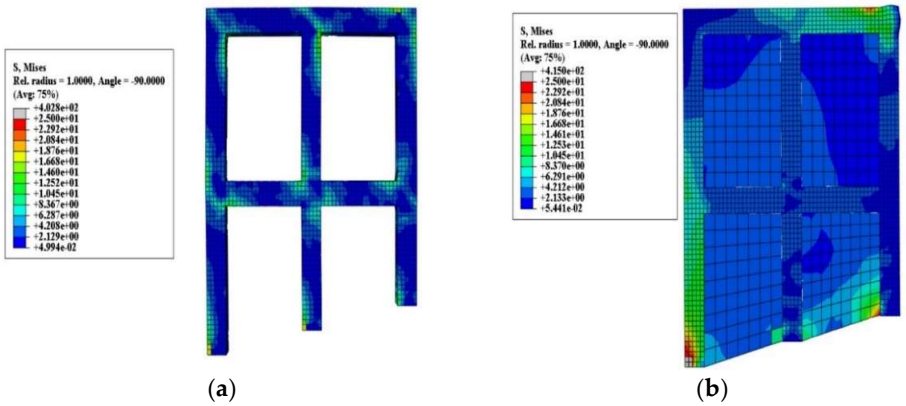



**Figure 12.** Von mises stress pattern for reinforced concrete frames. (**a**) Bare frame (**b**) Infilled frame.

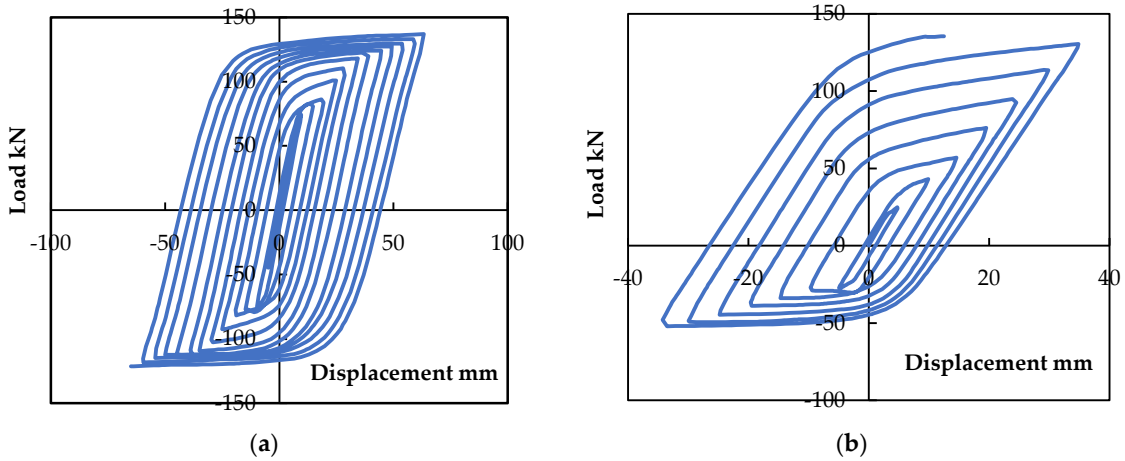



**Figure 13.** Hysteretic curve for a reinforced concrete sloped frame. (**a**) Bare frame. (**b**) Infill frame.

There is a comparison of the analytical and experimental results in Figure 14 and Table 3. It has been noted that there has been little difference between them. The discrepancy between the experimental inquiry and the analytical investigation in the bare frame is 1.9 kN. Furthermore, the displacement is the same for both the bare and Infill frame investigations. The finite element model replicates the fracture pattern found in the experimental study of the bare frame near support and joints in the same location as high-intensity stress deformation.

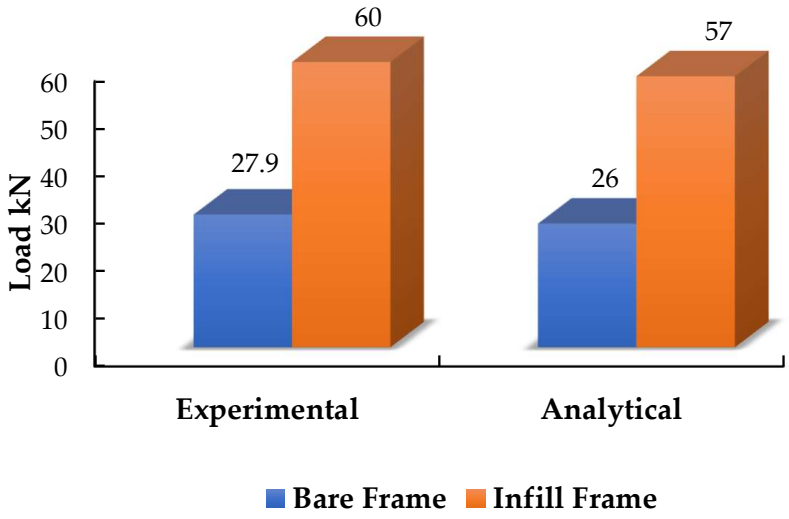



**Figure 14.** Comparison of the analytical and experimental data.

**Table 3.** Experimental and analytical data for the frames.

| Frame | Experimental | | Analytical | |
|---|---|---|---|---|
| | Load kN | Displacement mm | Load kN | Displacement mm |
| Bare Frame | 27.9 | 37 | 26 | 30 |
| Infill Frame | 60 | 13.1 | 57 | 14.5 |

The maximum principal stress observed on the reinforced concrete bare frame on the slope was 2.94 MPa in the critical region. The same stress deviates intensively and achieved 7.89 MPa in the critical region once the masonry infill is provided. Meanwhile, von mises stress is the measure of energy density based on all types of stresses in the specimen showing the failure of a ductile material. Von mises stress shows that stress intensity is predominant in the bare frame near supports and joints along with the region where the

short column effect is there, and the stress is around 4.9 Mpa. However, in the masonry infill frame, the stress intensity is very high at 5.44 MPa in the left end long column, along with the right bay masonry infill near the short column.

## 4. Conclusions

The effect of short column and infill on the seismic behaviour of the reinforced concrete frame was studied under lateral cyclic loading and the major findings are summarized as follows:

(i) When compared to reinforced concrete frames without infill, the displacement in frames with infill dramatically reduces. This occurs as a result of the addition of infill, which increases the frame's overall rigidity to handle the lateral stress.

(ii) The infilled frame's ultimate load-carrying capability against lateral cyclic stress is over 50% greater than the bare frame. The presence of solid infill in the short column zone greatly reduces rapid failure due to shear, and progressively increases the stiffness of the entire frame, allowing it to support twice the load.

(iii) The energy absorption capacity of the reinforced concrete frame with Infill is 2.45 times greater than that of the bare frame without infill. The energy absorption and dissipation capacity of the bare frame under lateral cyclic loading against the frame with infill are insignificant.

(iv) The maximum displacement of a bare frame is 37 mm at its ultimate load. Meanwhile, the displacement of the infilled frame is 13.1 mm at the same load. Therefore, the displacement of the in-filled frame is reduced exponentially.

(v) The initial crack was observed in the bare frame at 8 kn. whereas, in the infilled frame, the crack developed gradually at 14 kN. This shows that the provision of solid infill in a reinforced concrete frame with a short column effect leads to a significant change in the behaviour of the reinforced concrete frame in resisting lateral load by improving deformation capacity, as well as the stiffness of the frame in total, irrespective of the short column effect.

(vi) The hysteresis loop of the bare frame shows a significant drop in the slope after the maximum load. On the other side where the masonry infill is provided the decreasing of slope takes place gradually after concrete failure. A building's capacity to withstand an earthquake is largely dependent on a significant degree on its capacity to disperse the energy input. The structure's capability is shown by its energy dissipation capacity to function effectively inside the inelastic range. The area below the bare frame loop is very less when compared to that of the infilled frame, which shows that the frame with masonry infill significantly dissipates the energy.

(vii) Von mises stress reflects the capacity of the infilled frame in dissipating energy under lateral load by shifting the stress from short columns to the infill and leading the column to withstand the sudden failure in the inelastic region. Hence the overall performance of the short column frame with infill improved due to the global retrofitting technique.

**Author Contributions:** P.S.: conceptualised the model and established the empirical theorem and conducted the experiment. S.S.S. and S.K.S.: supervised the research, as well as the analysis of the results. P.S. introduced the idea of cyclic loading to this project and wrote the paper and performed the review and submission: S.S.S., S.K.S., B.G.A.G. and K.R.: collaborated on and coordinated the research. B.G.A.G. and K.R.: suggested and chose the journal for submission. P.S., S.S.S., S.K.S., B.G.A.G. and K.R.: participated in the manuscript revision phase. All authors have read and agreed to the published version of the manuscript.

**Funding:** This research received no external funding.

**Institutional Review Board Statement:** Not applicable.

**Informed Consent Statement:** Not applicable.

**Data Availability Statement:** The data presented in this study are available on request from the corresponding author.

**Conflicts of Interest:** This manuscript has not been submitted to, nor is it under review at, another journal or other publishing venue. The authors have no affiliation with any organization with a direct or indirect financial interest in the subject matter discussed in the manuscript. The authors declare no conflict of interest.

## References


1. Woodward, K.A.; Jirsa, J.O. Influence of Reinforcement on RC Short Column Lateral Resistance. *Eng. Struct.* **1984**, *110*, 90–104. [CrossRef]
2. Chung, Y.S.; Meyer, C.; Shinozuka, M. *Seismic Damage Assessment of Reinforced Concrete Members*; Report NCEER-87-0022; National Center for Earthquake Engineering Research, State University of New York: Buffalo, NY, USA, 1987.
3. Paul, D.; Kumar, S. Stability analysis of slope with building loads. *Soil Dyn. Earthq. Eng.* **1997**, *16*, 395–405. [CrossRef]
4. Sivaselvan, M.V.; Reinhorn, A.M. *Hysteretic Models for Cyclic Behavior of Deteriorating Inelastic Structures*; Technical Report NCEER-99-0018; National Center for Earthquake Engineering Research, State University of New York: Buffalo, NY, USA, 1999.
5. Promis, G.; Ferrier, E.; Hamelin, P. Effect of external FRP retrofitting on reinforced concrete short columns for seismic strengthening. *Compos. Struct.* **2009**, *88*, 367–379. [CrossRef]
6. Cagatay, I.H.; Beklen, C.; Mosalam, K.M. Investigation of short column effect of RC buildings: Failure and prevention. *Comput. Concr.* **2010**, *7*, 523–532. [CrossRef]
7. Pradeep, S.; Dinakar, P.; Satyanarayanan, K. Study on Dynamic Characteristics of Infilled Frames with Pneumatic Interface. *Mater. Today Proc.* **2019**, *14*, 257–263. [CrossRef]
8. Singh, Y.; Gade, P.; Lang, D.H.; Erduran, E. 2012. Seismic Behavior of Buildings Located on Slopes-An Analytical Study and Some Observations From Sikkim Earthquake of September 18, 2011. In Proceedings of the 15th World Conference on Earthquake Engineering, Lisbon, Portugal, 24–28 September 2012. Available online: https://www.iitk.ac.in/nicee/wcee/article/WCEE2012_4201.pdf (accessed on 1 December 2022).
9. Khadiranaikar, R.B.; Masali, A. Seismic Performance of Buildings Resting on Sloping Ground. In *Advances in Structural Engineering*; Springer: New Delhi, India, 2014; pp. 803–813. [CrossRef]
10. Pradeep, S.; Kunal, P. Analytical Study of Seismic Behaviour of RCC Frame with Short Column Effect. *Int. J. Civ. Eng. Technol.* **2017**, *8*, 362–372.
11. Xue, W.; Hu, X. Seismic performance of a four-story two-bay high-performance concrete frame under low reversed cyclic loading. *KSCE J. Civ. Eng.* **2017**, *21*, 2707–2716. [CrossRef]
12. Ganesan, N.; Indira, P.; Irshad, P. Effect of ferrocement infill on the strength and behavior of RCC frames under reverse cyclic loading. *Eng. Struct.* **2017**, *151*, 273–281. [CrossRef]
13. Satyanarayanan, K.; Varshini, R.; Pradeep, S. Feasibility Studies on Proactive Disaster Prevention in frames of sloped regions. *Mater. Today Proc.* **2019**, *14*, 315–322. [CrossRef]
14. Karami, F.; Izadpanah, M. Incremental inelastic dynamic damage analysis of MRRCFs infilled with masonry panels. *J. Build. Eng.* **2021**, *44*, 103282. [CrossRef]
15. Pachappoyil, N.S.; Agarwal, P. Performance evaluation of the energy dissipating hysteretic infill wall frame considering opening under in-plane and out-of-plane loading. *Eng. Struct.* **2021**, *249*, 113329. [CrossRef]
16. Sarangapani, G.; Venkatarama Reddy, B.V.; Jagadish, K.S. Brick-mortar bond and masonry compressive strength. *J. Mater. Civ. Eng.* **2005**, *17*, 229–237. [CrossRef]
17. Ruggieri, S.; Fiore, A.; Uva, G. A New Approach to Predict the Fundamental Period of Vibration for Newly-designed Reinforced Concrete Buildings. *J. Earthq. Eng.* **2021**, *26*, 6943–6968. [CrossRef]
18. Maruthish, K.; Satyanarayanan, K.; Pradeep, S.; Muthukumar, S. Study on infilled frames with partial interface materials under inplane monotonic loading. *Mater. Today Proc.* **2021**, *43*, 3256–3260. [CrossRef]
19. Muthukumar, S.; Satyanarayanan, K.S.; Senthil, K. Studies on two bay and three storey infilled frame with different interface materials: Experimental and finite element studies. *Struct. Eng. Mech* **2017**, *64*, 543–555.
20. Foti, D. Response of frames seismically protected with passive systems in near-field areas. *Int. J. Struct. Eng.* **2014**, *5*, 326. [CrossRef]
21. Kumar, S.M.; Saranya, G.; Lakshmipathy, M.; Satyanarayanan, K.S. Modeling and Study of Behavior of Infilled Frames with Diferent Interface Materials under Static Loading. *Indian J. Sci. Technol.* **2016**, *9*, 1–6.
22. *IS 383*; Specification for Coarse and Fine Aggregates from Natural Sources for Concrete. Bureau of Indian Standards: New Delhi, India, 1970; pp. 1–24.
23. *IS 456*; Plain Concrete and Reinforced. Bureau of Indian Standards: New Dehli, India, 2000; pp. 1–114.
24. *IS 12269*; Ordinary Portland Cement, 53 Grade—Specification. Bureau of Indian Standards: New Dehli, India, 1987; pp. 1–17.
25. *IS 516*; Method of Tests for Strength of Concrete. Bureau of Indian Standards: New Delhi, India, 1959; pp. 1–30.
26. *ABAQUS Standard User's Manual*; Dassault Systèmes, Version 6.10, USA. The Abaqus Software is a product of Dassault Systèmes Simulia Corp.: Providence, RI, USA, 2010.

27. Hu, P.; Liu, Y.; Wang, J.; Wang, W.; Pan, G. Experimental Investigation and Numerical Analyses on Cyclic Behavior of the Prefabricated Concrete Frame Infilled with CFS-CLPM Composite Walls. *Buildings* **2022**, *12*, 1991. [CrossRef]
28. Ali, E.; Althoey, F. Numerical Investigation on Blast Response of Cold-Formed Steel Framing Protected with Functionally Graded Composite Material. *Buildings* **2022**, *12*, 118. [CrossRef]

**Disclaimer/Publisher's Note:** The statements, opinions and data contained in all publications are solely those of the individual author(s) and contributor(s) and not of MDPI and/or the editor(s). MDPI and/or the editor(s) disclaim responsibility for any injury to people or property resulting from any ideas, methods, instructions or products referred to in the content.